Mo-based coatings with anti-wetting properties for high temperature applications: Synthesis by plasma technology

James Aluha[1], Marie-Claude Fournier[1], Faranak Barandehfard[1], Pierre-Olivier Langlois[1], Kossi Béré[1], Nicolas Abatzoglou[1], and François Gitzhofer[1]

[1]*Department of Chemical & Biotechnological Engineering, Université de Sherbrooke, Sherbrooke (QC), Canada, J1K 2R1*

Abstract: Coatings composing Mo and Al-Mo deposited on Fe-based substrates were produced at high temperature using a radio frequency (RF) suspension plasma spray (SPS) system. Characterization of the materials by Microscopy (SEM) and X-ray diffraction (XRD) revealed that the coatings were completely metallic, with no carbides or metal oxides detected. ALCAN's standard "immersion" test performed at 850ºC for 96 hours proved the unique anti-wetting properties of Mo when immersed in molten aluminium-magnesium alloy.

Keywords: SPS, induction plasma technology, molybdenum, anti-wetting, coatings

1. Introduction

Global demand for aluminium is continuously increasing and according to the International Aluminium Institute (IAI), the 2018 output totalled 64.34 million tonnes, most of which goes through the sow moulds to produce ingots. In sow casting, the liquid Al is transferred from ladles into large steel moulds where the molten metal cools and solidifies. Pyrotek® indicates that the sows are sold for remelting in secondary aluminium processes and optimized production efficiency depends on mould lifetime, solidification time, mould release, ingot quality and reduced scrap.

Since aluminium has a tendency to stick onto other metals, a coating of boron nitride is spray painted to cover the sow moulds in order to prevent the molten Al from sticking. However, this coating has to be done every time, and the process becomes tedious. Therefore, a permanent solution would be to use a plasma-sprayed coating with non-wetting characteristics towards molten Al and Al-Mg alloys. Besides the chemistry of the materials in contact, some of the factors that exacerbate wetting are high surface roughness, sample porosity, and chemical reactions that lead to a low contact angle with the molten Al [1].

As shown in **Figure 1**, the wettability of a solid surface is a function of its contact angle with the wetting liquid.

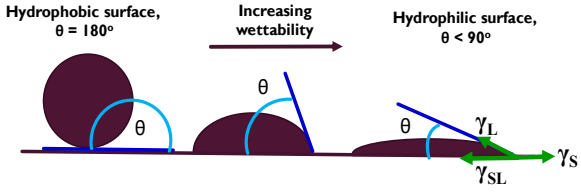

Fig. 1. The wettability of a solid surface.

Therefore, wettability is determined by Young's equation:

$$\gamma_S = \gamma_{SL} + \gamma_L Cos\theta \qquad (1)$$

where γ_S is the solid surface energy; γ_{SL} is the solid–liquid interfacial energy; and γ_L is the surface tension defined by the liquid–vapor interfacial energy.

In order to improve the anti-stick properties of coating materials used in Al extraction, its contact angle with molten Al should increase, and some anti-wetting additives have been shown to improve the contact angle by between 105 and 125º [1].

Therefore, the objective of this work is to produce Mo-rich coatings deposited on iron-based substrates, which can protect the metallic components used in Al extraction. Inductive suspension plasma spray (SPS) technology is the method of choice in synthesizing the coatings since metal powders are dispersed in a viscous fluid and the suspension injected into the plasma. The suspension approach is preferred because it introduces flexibility that aids in modifying various compositions during the preparation of coatings with composite metal formulations.

Although traditional methods such as physical or chemical vapor deposition produce nano-structural coatings of good mechanical and physical properties [2], the evolution of SPS technology is perceived to mitigate the slow application speed and the high process costs involved. However, in order to guarantee stable particle atomization, the SPS technique requires high mass ratio between the plasmagenic gas and the injected suspension. Bigger suspension mass depresses fluid vaporization and cools the plasma, resulting in coatings having some unmolten particles [3]. This leads to poor coating structure, besides a general low injection efficiency, but proper plasma jet design can fix these impediments.

2. Experimental Methods

In this work, low-pressure plasma spraying is employed. A thin film from Mo metal (purity 99.95%) with particle size 2 – 4 µm, and Al metal (purity 99.9%) of particle size 1 – 5 µm were deposited on iron-based substrates. The SPS system whose design and setup is illustrated in **Figure 2** operates at 3.2 MHz alongside other system parameters,

using the PL-50 plasma torch with a supersonic nozzle supplied by Tekna Inc.

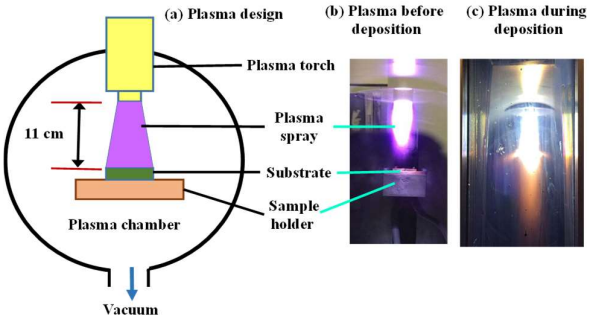

Fig. 2. Illustrated plasma design, with some pictures displaying the SPS system during operation.

A homogeneous mixture of 46.9 g metal (Mo only, 2.4 g Al + 44.5 g Mo, or 8.2 g Al + 38.7 g Mo) was dispersed in 53.1 g of ethlylene glycol ($C_2H_6O_2$) with a boiling point of 197.6°C. Due to laminar gas flow limitations in the plasma, the mixture was stirred for over 24 h before being injected into the plasma. Gas flow rates (in standard litres per minute, SLPM) included sheath gas (Ar = 78; H_2 = 6.5; and N_2 = 22), central gas (Ar = 21), and carrier gas for powder injection (Ar = 10). The initial chamber pressure was 16 kPa, and in each deposition, two different substrates (cast iron and stainless steel) were sprayed concurrently for comparison purposes. **Table 1** provides a summary of the operational settings of the plasma system.

Table 1. Plasma settings for the deposition of pure Mo and Al-Mo coatings on Fe-based substrates.

Plasma power		40 kW
Total gas flow rate		137.5 SLPM
Suspension (solid in liquid)	Metal mass	46.9 g
	Ethylene glycol	53.1 g
Total suspension flow rate		2 $cm^3.min^{-1}$
Chamber pressure		16 kPa
Deposition distance		11 cm
Sample pre-treatment		35 cycles
Deposition		50 cycles
Deposition time per cycle		4 s

The suspension composition was thermodynamically determined by phase-diagrams. Modelling by FactSage thermodynamic software as seen in **Figure 3** showed that Al-Mo alloy coatings must contain over 75% Mo (mol/mol) in order to operate above 1000°C [4]. In this project, the Al–Mo binary system is considered as a strategic system for the development of functional Mo-rich aluminides [5].

Table 2 shows among other properties of the materials used in this work, the linear thermal expansion coefficients, which describe the relative change in the length of a material per degree temperature change. It is clear that the dimensional change in Al (23.1 x 10^{-6} K^{-1}) is almost twice that of the Fe (11 x 10^{-6} K^{-1}), which is in turn nearly twice as that of Mo (4.8 x 10^{-6} K^{-1}). In order to obtain an intermediate thermal expansion coefficient between that of pure Mo and Fe, an inclusion of 10% Al was made into Mo, since earlier works have indicated that increasing the mass of another metal in order to create Al alloys alters the expansion coefficients linearly [6]. Therefore, the thermal expansion coefficient of the envisaged coating is most likely to increase linearly to about 9 if the Al added to Mo does not exceed 25% according to FactSage thermodynamic data [4].

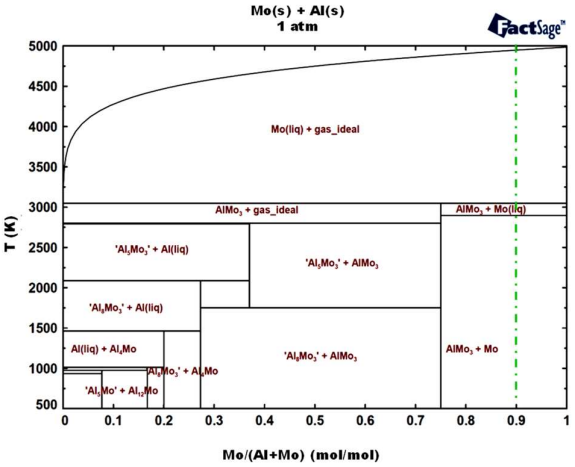

Fig. 3. The predicted Al-Mo phase diagram using FactSage thermodynamics [4].

Table 2. Physical properties of the materials used in this work.

Material's property	Substrate		Coating	
	Cast Iron	Steel	Al	Mo
Atomic number	26 (Fe)		13	42
Atomic mass	55.85 (Fe)		26.98	95.95
Density (g/cm^3)	6.80	7.80	2.70	10.28
Melting point (°C)	1150	1538	660	2623
Boiling point (°C)	-	2862	2470	4639
Crystal structure[#]	BCC	BCC	FCC	BCC
CTE* (10^{-6}/K)	10.5	11.0	23.1	4.8
Young's modulus (GPa)	165	210	70	329

[#] Ambient conditions (25°C)
* CTE = Coefficient of linear thermal expansion at 25°C

In the proposed Al-Mo coating, having a high Young's modulus value for Mo (329 GPa) will compensate for the low value in Al (70 GPa), which means that the coating will not easily deform during high temperature operations. In addition, since the Al has face-centred cubic (FCC) crystal structure, it was intended to enhance the adhesion of Mo to the Fe substrate. Mo has body-centred cubic (BCC) crystal structure, while Fe displays the FCC crystal structure (austenite) at high temperatures, but converts to the BCC crystal structure (pearlite) at low temperatures.

After synthesis, the samples were characterized by imaging on a scanning electron microscope (SEM, Hitachi S-4700), coupled with energy dispersive X-ray (EDX) spectroscopy and elemental X-ray mapping. Phase analysis by X-ray diffraction (XRD) was conducted on a PANalytical Philips X'pert PRO Diffractometer set in the Bragg-Brentano configuration with proportional Xe point detector. The instrument is fitted with Ni-filters for the Cu Kα radiation produced at 40 kV and 50 mA, wavelength alpha1 (λ = 1.540598Å) and was operated on the factory-installed Analytical Data Collector software.

The anti-wetting properties and corrosion resistance of pure Mo in contact with molten Al-5182 aluminium-magnesium alloy (5%Mg/Al), were evaluated through the ALCAN's standard "immersion" test performed at 850°C for 96 h, and imaging of the sample surface after the test was done on a Keyence VHX-5000 optic microscope.

3. Results and Discussion

Sample analysis using SEM imaging indicated complete coverage of the substrate by the deposited metal coating, as exemplified in **Figure 4**, which shows splats of pure Mo metal deposited on cast iron. The shape of the splats normally depend on many factors such as the substrate's topology and physical properties, droplet size, velocity, gas particle trajectories and other thermos-physical properties of the impacting particles [7]. Some authors have shown that in the production of molybdenum splats and coatings, Young's modulus, hardness and thermal conductivity increase with particle velocity, while oxygen content and porosity decrease [8]. Subsequently, in this work, the total plasma gas flow rate was set at ~140 SLPM to achieve high particle velocities.

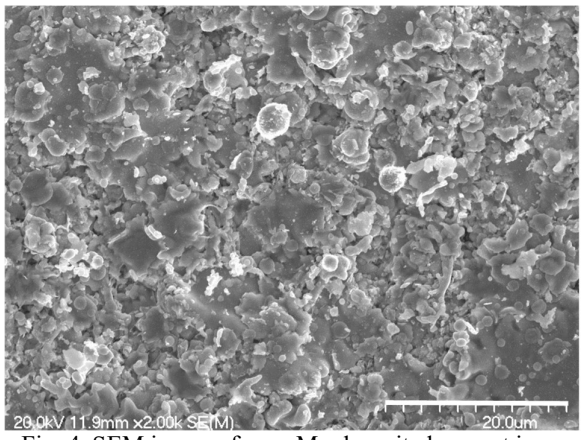

Fig. 4. SEM image of pure Mo deposited on cast iron.

One of the successes of the approach used in this project is that although ethylene glycol was used to deliver the suspension into plasma, there were no traces of residual carbon deposited, metal-carbides nor metal-oxides in the final coatings as indicated from the XRD spectra given in **Figure 5**. In both the Mo-only sample and the Al-Mo alloy, an intense peak at 41° [2θ]-angle was observed, alongside two other peaks at 59° and 74°, which are reflections of the (110), (200) and (211) planes respectively, and they signify the presence of metallic Mo in the coatings.

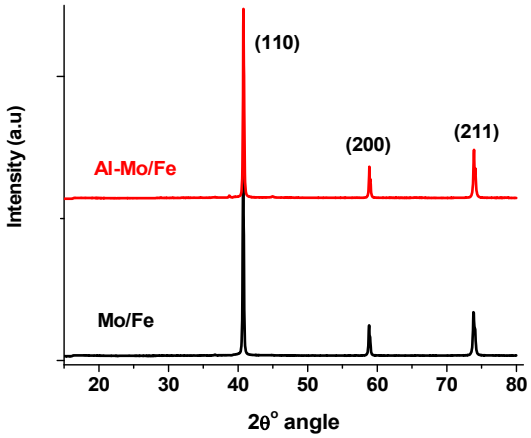

Fig. 5. Absence of metal carbides and oxides confirmed by XRD patterns of 10%Al-90%Mo coatings on cast iron.

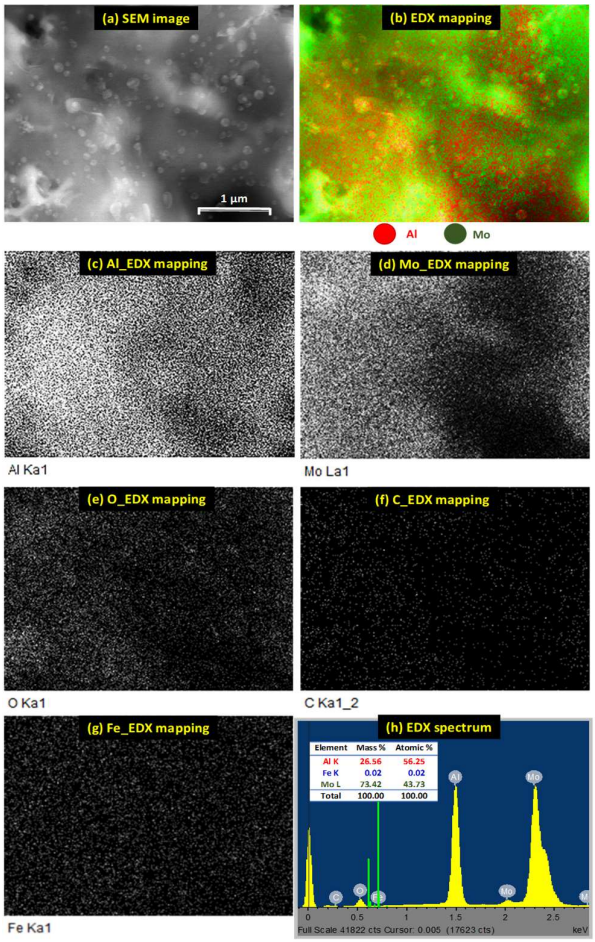

Fig. 6. SEM imaging with EDX elemental mapping of the 44%Al-56%Mo coating on stainless steel.

Figure 6(a) shows the secondary electron image of the 44%Al-56%Mo/Fe sample coated on steel. Images that follow represent the elemental EDX-mapping of each element. The mixer image in **Figure 6(b)** shows uniform distribution of both Al and Mo in the coating; **(c)** displays Al only; **(d)** depicts Mo only; **(e)** shows the absence of oxides generally, and **(f)** indicates the absence of metal carbides or carbon deposition. **Figure 6(g)** indicating no iron detected on the surface revealed that the substrate was completely covered by the coating. The EDX spectrum in **Figure 6(h)** established the Al:Mo elemental ratio of about 44:56 (mol.%) in the material as expected. The small oxygen signal observed in the EDX spectrum is surface oxygen, which is not associated with any particular metal.

Figure 7 indicates why with accelerated particle cooling, the production of Mo-carbides and Mo-oxides above 2000°C was remote. Since the velocity of the plasmagenic gases is very high, there is no time for the formation of oxides or carbides below the quench line (dotted vertical line at 2000°C).

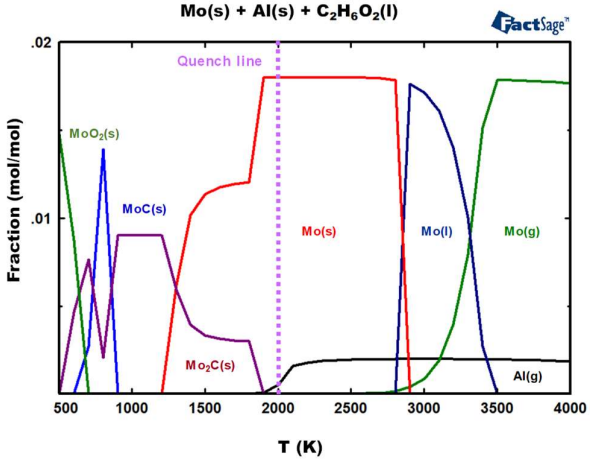

Fig. 7. FactSage simulating the possible plasma products formed in the Al-Mo coating [4].

Images from an optic microscope revealed the anti-wetting properties of Mo in molten Al-Mg alloy, evidenced from ALCAN's standard "immersion" test performed at 850°C for 96 h, see **Figure 8(a)**. After cooling, the Al-Mg alloy peeled off easily without sticking on the surface of the Mo sample as depicted in **Figure 8(b)** and **(c)**.

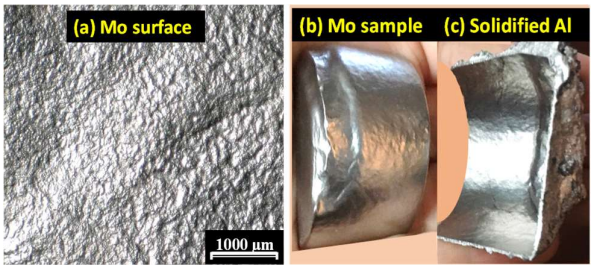

Fig. 8. Anti-wetting properties: clean separation of Mo surface from molten Al-5%Mg alloy after ALCAN's standard "immersion" test for 96 h.

From this preliminary study, it was observed that both substrates (cast iron and stainless steel) can produce decent anti-wetting Mo and Al-Mo coatings. Our findings are in agreement with some authors who have achieved good metallurgical bonding between a Mo-containing coating and the surface of 45 steel substrate [9].

4. Conclusion

In this work, we report the successful deposition of metallic Mo coating on cast iron and stainless steel through high temperature suspension plasma-spray technology. Microscopic (SEM) imaging, coupled with elemental mapping by EDX analysis in addition to XRD analysis revealed that both the Mo/Fe and Al-Mo/Fe coatings did not contain any residual carbon or carbides; and neither did the thermal deposition process create metal oxides. Preliminary results from the ALCAN's standard "immersion" test indicated that Mo had exceptional anti-wetting properties towards molten Al-5%Mg alloy. Future work will involve the development of other Mo-based formulations with improved anti-wetting properties.

5. Acknowledgements

We thank ALCOA, Centre québécois de recherche et de développement de l'aluminium (CQRDA), Mitacs, Natural Sciences and Engineering Research Council of Canada (NSERC), and Pyrotek Inc., for financial support.

6. References

[1] A. Yurkov, Refractories for Aluminum, Electrolysis and the Cast House, Springer International Publishing, Moscow, Russia, p.278 (2017).

[2] V. Astié, C. Millon, J.-M. Decams and A. Bartasyte, in: Chemical Vapor Deposition for Nanotechnology, P. Mandracci (Editor), IntechOpen, London (UK), p.29 (2018).

[3] L. Latka, S.B. Goryachev, S. Kozerski and L. Pawlowski, Materials, **3**, 3845 (2010).

[4] C.W. Bale, E. Bélisle, P. Chartrand, S.A. Decterov, G. Eriksson, A.E. Gheribi, K. Hack, I.H. Jung, Y.B. Kang, J. Melançon, A.D. Pelton, S. Petersen, C. Robelin, J. Sangster and M.-A. Van Ende, FactSage Thermochemical Software and Databases, 2010-2016, Calphad, **54**, 35 (2016).

[5] M.J. Kriegel, A. Walnsch, O. Fabrichnaya, D. Pavlyuchkov, V. Klemm, J. Freudenberger, D. Rafaja and A. Leineweber, Intermetallics, **83**, 29 (2017).

[6] P. Hidnert and H.S. Krider, Journal of Research of the National Bureau of Standards, **48**, 209 (1952).

[7] J. Mostaghimi and S. Chandra, Pure and Applied Chemistry, **74**, 441 (2002).

[8] S. Sampath, X. Jiang, A. Kulkarni, J. Matejicek, D.L. Gilmore and R.A. Neiser, Materials Science and Engineering A, **348**, 54 (2003).

[9] K. Wang, B. Chang, J. Chen, H. Fu, Y. Lin and Y. Lei, Applied Sciences, **7**, 1065 (2017).